

Energy harvesting in silicon optical modulators

Sasan Fathpour and Bahram Jalali

Optoelectronic Circuits and Systems Laboratory
Electrical Engineering Department
University of California, Los Angeles, CA, 90095 USA
sasan@ee.ucla.edu, jalali@ucla.edu

<http://www.ee.ucla.edu/~oeecs/>

Abstract: An electro-optic silicon modulator with negative electrical power dissipation is proposed. The device performs optical modulation through electrical control of losses caused by two photon absorption. It further exploits the nonlinear photovoltaic effect to recover the optical power that is normally dissipated when the modulator is in the on state.

©2006 Optical Society of America

OCIS codes: (230.7370) Waveguides; (250.3140) Integrated optoelectronic circuits; (350.6050) Solar energy.

References and links

1. R. A. Soref, "Silicon-based optoelectronics," Proc. IEEE **81**, 1687-1706 (1993).
2. L. Pavesi, and G. Guillot, ed., *Optical interconnects: the Silicon approach* (Springer Series in Optical Sciences, 2006; ISBN: 3540289100).
3. D. J. Frank, "Scaling CMOS to the Limits," IBM J. Research and Development **46**, 235-244 (2002).
4. International Technology Roadmap for Semiconductors, 2005 Edition, <http://www.itrs.net/>.
5. S. Fathpour, K. Tsia, and B. Jalali, "Photovoltaic Effect in Silicon Raman Amplifiers," in *Optical Amplifiers & Their Applications Conf.*, (Optical Society of America, Washington, D.C., 2006), paper PD1.
6. S. Fathpour, K. K. Tsia, and B. Jalali, "Energy harvesting in silicon Raman amplifiers," Appl. Phys. Lett. **89**, 061109 (2006).
7. B. Jalali, S. Fathpour, and K. K. Tsia, "Energy Harvesting in Silicon Photonic Devices," *LEOS Annual Meeting 2006*, (Institute of Electrical and Electronics Engineers, New York, 2006).
8. A. Irace, G. Breglio, M. Iodice, and A. Cutolo, "Light modulation with silicon devices," in *Silicon Photonics*, L. Pavesi, and D. J. Lockwood, ed. (Springer-Verlag, 2004).
9. L. Liao, D. Samara-Rubio, M. Morse, A. Liu, D. Hodge, D. Rubin, U. D. Keil, and T. Franck, "High speed silicon Mach-Zendher modulator," Opt. Express **13**, 3129-3135 (2005).
10. A. Huang, C. Gunn, G. Li, Y. Liang, S. Mirsaidi, A. Narasimha, and T. Pinguet, "A 10Gb/s photonic modulator and WDM MUX/DEMUX integrated with electronics in 0.13 μ m SOI CMOS," *International Solid-State Circuits Conference (ISSCC 2006) Digest of Technical Papers* (Institute of Electrical and Electronics Engineers, New York, 2006), pp. 245-246.
11. Q. Xu, B. Schmidt, S. Pradhan, and M. Lipson, "Micrometre-scale silicon electro-optic modulator," Nature **435**, 325-326 (2005).
12. R. A. Soref, and B. R. Bennett, "Kramers-Kronig analysis of E-O switching in silicon," *SPIE Integr. Opt. Circuit Eng.*, SPIE **704**, 32-37 (1986).
13. R. Claps, V. Raghunathan, D. Dimitropoulos, and B. Jalali, "Influence of nonlinear absorption on Raman amplification in Silicon waveguides," Opt. Express **12**, 2774-2780 (2004).
14. D. Dimitropoulos, R. Jhaveri, R. Claps, J. C. S. Woo, and B. Jalali, "Lifetime of photogenerated carriers in silicon-on-insulator rib waveguides," Appl. Phys. Lett. **86**, 071115 (2005).
15. A. Irace, G. Breglio, and A. Cutolo, "All-silicon optoelectronic modulator with 1GHz switching capability," Electron. Lett. **39**, 232-233 (2003).
16. V. R. Almeida, C. A. Barrios, R. R. Panepucci, M. Lipson, M. A. Foster, D. G. Ouzounov, and A. L. Gaeta, "All optical switch on a silicon chip," in *Proceedings of Conference on Lasers and Electro-optics, CLEO 2004*, Institute of Electrical and Electronics Engineers, New York, 2004).
17. R. L. Espinola, J. I. Dadap, R. M. Osgood, Jr., S. J. McNab, and Y. A. Vlasov, "Raman amplification in ultrasmall silicon-on-insulator wire waveguides," Opt. Express **12**, 3713-2718 (2004).

1. Introduction

Silicon-on-insulator (SOI) has been long envisaged as a platform for integration of photonics and CMOS-based VLSI circuits [1]. Such a technology may offer a solution to the interconnect problem in computer systems, as well as producing low-cost optical transceivers for local area and long-haul optical networks. Much progress has been made towards low-loss silicon waveguides, photodetectors, electro-optic modulators, light emitting diodes and Raman lasers and amplifiers [2]. However, little or no attention has been made to the power dissipation of Si photonic devices.

Heating and thermal management is the central problem faced by the VLSI industry. The problem is so severe that it threatens to bring to halt the continued advance of VLSI as described by Moore's law [3]. This is highlighted by the recent momentous shift of the microprocessor industry away from increasing the clock speed and in favor of multi-core processors [4]. This suggests that the power dissipation of Si photonic devices is an important concern for their integration with VLSI electronics.

Typically, the most power-hungry photonic devices are the laser. However, the lack of an electrically-pumped Si laser, to date, dictates an architecture where the light source remains off-chip. In such architecture, an off-chip source powers the chip, whereas modulators, amplifiers, photodetectors, and perhaps wavelength converters, are integrated on the chip. We have recently demonstrated two-photon photovoltaic effect in Silicon Raman amplifiers [5-7], in which the energy of the pump beam lost to two-photon absorption (TPA) is harvested into useful net electrical power rather than being dissipated into heat. The present work addresses the power dissipation of silicon optical modulators and proposes a new type of modulator that exploits the same two-photon photovoltaic effect to achieve negative power dissipation.

2. Photovoltaic effect in silicon modulators

The free carrier plasma effect has been the most popular mechanism for achieving electro-optic modulation in silicon due to the lack of linear electro-optic effect in the material. The principle of operation is the modulation of free carrier density in which the optical loss and/or refractive index is modulated by injection, depletion, accumulation or inversion of free carriers. Numerous variations of the device have been reported, a review of which can be found elsewhere [8]. More recently reported devices include Mach-Zehnder modulators operating at 10 Gb/s, demonstrated with carrier accumulation in a MOS capacitor waveguide [9] and carrier depletion in a p-n junction waveguide [10], and the demonstration of carrier-injection modulation scheme in a p-n junction ring resonator [11].

In this work, we propose an electro-optic modulation approach that can offer electrical power generation (negative dissipation). The device generates electrical power by harvesting the optical power and is inspired by the solar cells. A solar cell, however, cannot perform optical modulation because the above bandgap photons are always absorbed by the semiconductor, regardless of the electrical bias. The proposed device combines the concept of a solar cell with nonlinear TPA in a silicon wire.

An implementation of the device is shown in Fig. 1(a), which consists of a SOI waveguide with a straddling p-n junction. The optical input frequency is below the absorption edge of silicon such that no linear absorption occurs. Although the device structure is similar to a conventional silicon optical modulator, the principle of its operation is entirely different. The input optical power and the wire cross-section are chosen such that the optical intensity is sufficiently high to induce TPA. The TPA-induced free carrier generation creates a current-voltage relation that resembles that of a solar cell (Fig. 1(b)). Such a device generates electrical power whenever the device is biased in the fourth quadrant. The TPA-generated carriers are swept out by the built-in field of the junction.

For the device to operate as an optical modulator with electrical power generation, then sufficient carrier modulation must be achieved while the device is entirely or partially in the fourth quadrant. Considering the example in Fig. 1(b), when the voltage is just below the turn-on voltage, carrier density is high and light is attenuated. To create the low attenuation state,

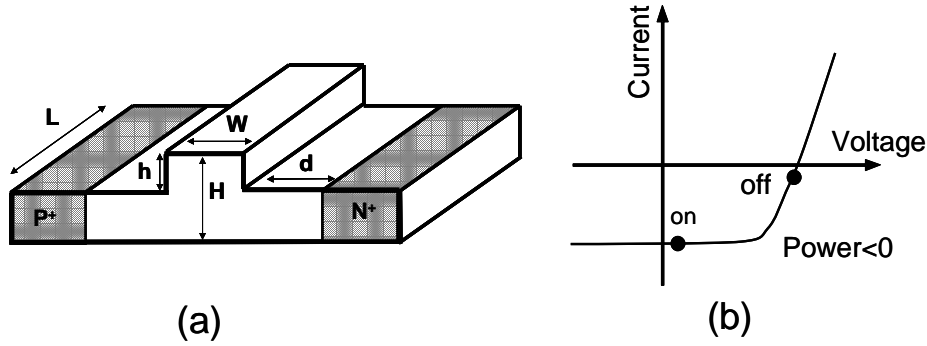


Fig. 1. (a) Schematic of the silicon electro-optical modulator with straddling p-n junction; the values of the shown geometrical dimensions used in the numerical simulations are: $H=0.3 \mu\text{m}$, $W=0.5 \mu\text{m}$, $h=0.25 \mu\text{m}$, $d=2 \mu\text{m}$, and $L=1 \text{ cm}$; (b) typical current-voltage characteristics of a photodiode under optical illumination, showing one choice of on and off states of the modulator in the fourth quadrant with negative power dissipation.

the bias is reduced leading to partial sweep-out of carriers as evident by the increase in the reverse current. From the above qualitative description, it is evident that there exists a tradeoff between the optical modulation depth and electrical power generation. On- and off-state voltages that are further apart result in larger modulation depths. However, the device becomes dissipative as the voltages move outside of the fourth quadrant. Another requirement is high optical intensities needed for TPA to occur. High intensities are achievable in Si wires, i.e., waveguide with scaled cross-sections. For example, in a waveguide with $0.15 \mu\text{m}^2$ modal area, the required optical intensity will be shown to be on the order of 50 mW. This relatively large power is generated by an off-chip laser, so it does not compromise the heating of the chip. Nevertheless, the requirement for high optical power is a tradeoff that one experiences in achieving negative on-chip electrical power dissipation.

In the next section, we quantify the performance of the proposed device using numerical simulations.

3. Model

The dependence of optical absorption on carrier density is given by the well-known expression of Soref [12]:

$$\alpha_{FCA} = \Delta\alpha_e + \Delta\alpha_h = 8.5 \times 10^{-18} \cdot \Delta N + 6.0 \times 10^{-18} \cdot \Delta P, \quad (1)$$

where ΔN and ΔP are the free electron and hole concentrations, respectively. In the presence of TPA, the propagation of optical intensity is given by the following nonlinear differential equation [13]:

$$\frac{dI_p(z)}{dz} = -(\alpha + \alpha_{FCA}(z))I_p(z) - \beta I_p^2(z), \quad (2)$$

where $\beta = 0.7 \text{ cm/GW}$ is the TPA coefficient and α is the linear absorption coefficient of the waveguide. The free carrier absorption term, α_{FCA} , is a function of the optical intensity, I_p , and bias voltage, V . Other third-order nonlinear optical effects such as Raman and Kerr are weaker than TPA and do not materially impact the performance of the device [13].

The device was simulated using a commercial drift-diffusion simulator (ATLAS by Silvaco International). TPA was emulated by specifying a carrier generation rate at the waveguide core, $G = dN/dt = -(1/2E)dI_p/dz = \beta I_p^2/2E$, where $E = 0.8 \text{ eV}$ is the photon energy. The values of electron and hole bulk recombination lifetimes were 3 and 10 μs , respectively. A surface recombination velocity of 200 cm/s was used for both types of carriers [14]. The doping levels of n^+ and p^+ regions were $1 \times 10^{19} \text{ cm}^{-3}$. The simulator provides carrier concentration as a function of V from which the output optical intensity and modulation depth are obtained using Eq. (1). The optical transmission and modulation depth of the intensity

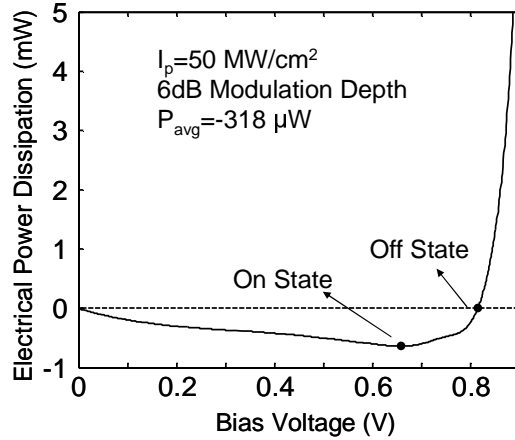


Fig. 2. Electrical power versus voltage characteristics of the optical modulator, showing biasing conditions with maximum attainable power generation in the on state and zero power dissipation in the off state.

modulator can be extracted from $I_p(L)/I_p(0)$ as a function of V . In order to accommodate for the three-dimensional (3-D) nature of the problem, a quasi-3D model was developed in which the 2-D results of ATLAS at several optical intensities are interpolated to numerically solve Eq. 2. The simulator also provides the diode current per unit length, J ($A/\mu m$), from which the

electrical power can be calculated from $P_{eff} = V \cdot I_{eff} = V \cdot \int_0^L J(I_p(z)) dz$. It is assumed in this

last expression that the ohmic loss of the contacts are negligible and that the current vector has no z -component. The latter is a fair approximation at low enough biases at which there is no voltage drop along the waveguide.

4. Results and discussions

Numerical simulations were performed for a silicon wire waveguide with an effective optical mode area of $0.15 \mu m^2$ and a length of 1 cm. The other geometrical dimensions are reported in the caption of Fig. 1(a). In order to achieve maximum power efficiency, the off-state was set at the minimum of the P - V characteristics and the on state was determined from the desired modulation depth. Figure 2 presents an example where the off state current is about zero and the average generated power, $P_{avg} = (P_{on} + P_{off})/2 = -318 \mu W$. The modulation depth is 6 dB for an input optical intensity of $50 MW/cm^2$. This corresponds to $V_{on} = 0.66 V$ and $V_{off} = 0.81 V$.

Figure 3(a) summarizes the tradeoff between the generated electrical power and the required input optical intensity. At sufficiently large signal intensities, the attainable P_{avg} can be as high as 1 mW while maintaining a modulation depth of 8 dB. To demonstrate the dependence on the modulating data format, we performed simulations for two extreme cases. One is a “digital” waveform corresponding to a binary signal with zero rise and fall times. The above-discussed P_{avg} corresponds to this digital case. The “sawtooth” case is a triangular waveform in which the generated power can be conveniently calculated from the average

swept power, $P_s = \int_{V_{on}}^{V_{off}} P dV / (V_{off} - V_{on})$. The generated power for a practical digital signal

with finite rise and fall times lies between these two extremes. The intensities required for zero power dissipation in both cases, i.e., intensities at which $P_{avg} = 0$ and $P_s = 0$, are presented in Fig. 3(b) versus modulation depth. It is evident that the required intensity for $P_s = 0$ is a factor of 1.8 to 2.3 smaller than the $P_{avg} = 0$ case.

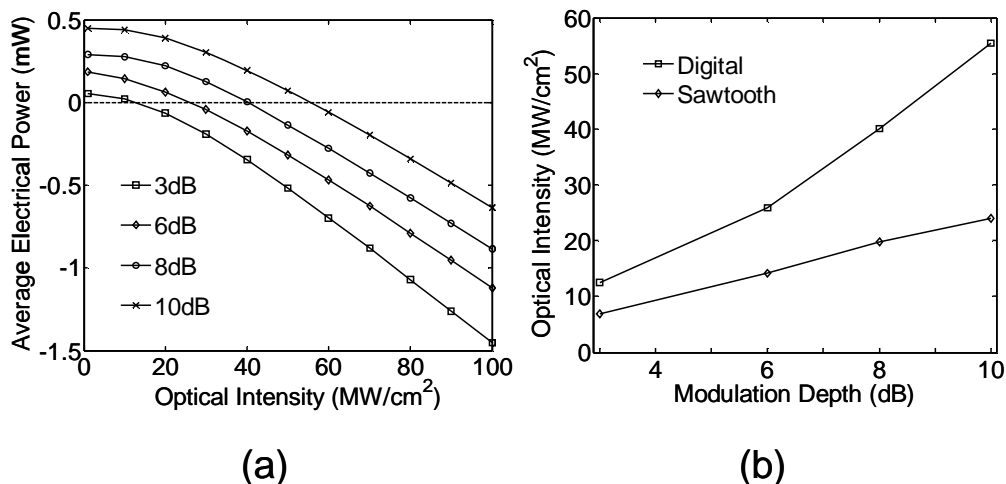


Fig. 3. (a) Average on-off power dissipation versus signal optical intensity at different modulation depths when the modulator is driving with an ideal digital waveform with zero rise/fall times; (b) optical intensity required for zero power dissipation for the digital waveform ($P_{avg} = 0$) and the sawtooth waveform ($P_s = 0$). For a practical digital waveform with finite rise and fall times, the power is between these two limits.

The above discussion considers a quasi-static case. We also performed transient simulations in order to include the charging and discharging of the diode capacitance. Simulations were performed with rise and fall times from 20 ps to 20 ns with data rates of 5-10 MHz. Classical switching transients at off-to-on and on-to-off transition edges were observed. The respective generated and dissipated transient powers of these transitions are almost equal. Hence, in the average of one period of the modulation, the electrical power is inconsiderably different than the discussed quasi-static case. It should be noted that the present simulations do not consider parasitic R , L , and C effects. These parameters depend on the specifics of device processing and packaging and are outside the scope of this paper.

Finally, although conventional carrier-injection modulators are considered to be slow with less than 100 MHz modulation bandwidth due to the large effective carrier recombination lifetime, over 1 GHz modulation bandwidths has been predicted with an optimized design in $1 \mu\text{m}^2$ optical mode area devices [15]. Even lower recombination lifetimes (~ 1 ns) is expected in wire waveguides [14], and has been experimentally reported [16], [17]. Therefore, modulation bandwidth comparable to depletion- and accumulation-based modulators [9], [10] is predictable for carrier-injection silicon wire modulators. It should be briefly noted that there exists a tradeoff between the modulation bandwidth and the generated electrical power, since reducing the effective lifetime decreases the collection efficiency of the photogenerated carriers. In practice, the lifetime can be optimized by controlling the surface recombination velocities [14] through passivation techniques.

5. Conclusions

Two-photon photovoltaic effect can be employed to harvest electrical energy from silicon photonic devices based on nonlinear optical effects, e.g., Raman and Kerr, in which two-photon absorption occurs. In this work, we have particularly explored the feasibility of energy harvesting in silicon wire electro-optic modulators. Negative electrical power dissipation as high as 1 mW is attainable in 1-cm long devices and for waveguides with $0.15 \mu\text{m}^2$ optical mode effective area with a digital non-return to zero modulating signal.

Acknowledgment

This material is based on research sponsored by DARPA.